

Synthesis of Anatase TiO_2 Tubular Structures Microcrystallites with a High Percentage of {001} Facets by a Simple One-Step Hydrothermal Template Process

Xiaoning Wang,^[a] Baibiao Huang,*^[a] Zeyan Wang,^[a] Xiaoyan Qin,^[a] Xiaoyang Zhang,^[a] Ying Dai,^[b] and Myung-Hwan Whangbo^[c]

Since the discovery of carbon nanotubes in 1991,^[1] tubular structures have received much attention.^[2–4] Owing to their special structures and outstanding mechanical/electrical properties, tubular structures have been widely used for the fabrication of microfluidics and optical devices, biomedical instruments, chemical microreactors, and composite materials.^[5–12] So far, various tubular structures have been produced by using vapor phase deposition, lamella structure scroll, template-assisted, metal-catalyst-assisted, and thermal solution methods.^[7,13–18] High-aspect-ratio TiO_2 nanotubular layers possess significantly stronger photocatalytic properties than nanoparticulate layers do.^[19] Thus, TiO_2 tubular materials are particularly interesting for their potential applications in photocatalysis and photovoltaic cells. TiO_2 crystals with {001} facets, which have a high surface energy and hence exhibit enhanced reactivity, are attractive as photocatalysts.^[20] Recently, a method to synthesize anatase TiO_2 single crystals with a high percentage of {001} facets has been developed,^[21] and has been used to prepare several morphologically different anatase TiO_2 materials with a high percentage of {001} facets and hence with high photocatalytic activities.^[22–24] So far, however, there has been no report on TiO_2 tubular materials exposing highly reactive {001} facets. In this work, we report a simple one-step hydrothermal method for preparing anatase TiO_2 tubular structures made up of microcrystallites with a high percentage of

{001} facets by using ZrO_2 fibers as a template. This process may provide a facile way to produce TiO_2 with special structures, which may have promising applications in photocatalysis and photoelectronics. Our analysis of the structures, morphologies, and growth procedures of the as-grown TiO_2 microtubes provides a plausible growth mechanism.

Figure 1 shows the XRD patterns of the as-grown samples obtained after hydrothermal processing at 200°C with a ZrO_2 template for various reaction times t . The products obtained with $t=6$ h exhibit a mixed phase of anatase TiO_2 (JCPDS card 21-1272) and tetragonal ZrO_2 (JCPDS card 79-1764, Figure 1b). The peaks corresponding to tetragonal ZrO_2 gradually decreases with increasing the reaction time t .

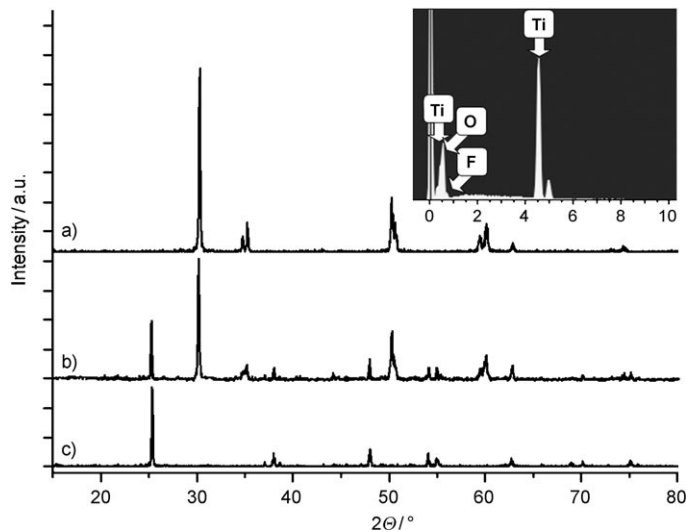


Figure 1. XRD patterns of a) the ZrO_2 template, b) the TiO_2 tubular structures obtained from hydrothermal processing at 200°C for $t=6$ h, and c) the TiO_2 tubular structures obtained from hydrothermal processing at 200°C for $t=24$ h. The inset shows the EDS of as-grown TiO_2 tubular structures obtained with $t=24$ h.

[a] X. Wang, Prof. Dr. B. Huang, Dr. Z. Wang, X. Qin, Prof. X. Zhang

State Key Lab of Crystal Materials
Shandong University, Jinan 250100 (China)

Fax: (+86) 531-8836-5969
E-mail: bbhuang@sdu.edu.cn

[b] Prof. Dr. Y. Dai

School of Physics
Shandong University, Jinan 250100 (China)

[c] Prof. Dr. M.-H. Whangbo

Department of Chemistry, North Carolina State University
Raleigh, North Carolina 27695-8204 (USA)

When $t=24$ h, the tetragonal ZrO_2 phase completely disappears, and all the diffraction peaks of the as-grown samples can be indexed to pure anatase TiO_2 (Figure 1c). This observation is further confirmed by the energy dispersive spectrum (EDS) of the as-grown TiO_2 tubular structures (see the inset of Figure 1); only Ti, O, and F atoms are detected from the as-grown TiO_2 samples with the $[\text{Ti}]/[\text{O}]$ ratio of 1:2.35, which is close to the expected stoichiometry. The presence of F is attributed to the presence of $(\text{NH}_4)\text{TiF}_6$ in the hydrothermal process.

Polycrystalline ZrO_2 fibers are long with smooth surfaces (Figure 2a), whereas the as-grown TiO_2 tubular structures are short ($70\text{--}150\ \mu\text{m}$) with rough surfaces (shown in Figure 2b). The SEM images in Figure 3 show zoomed-in views

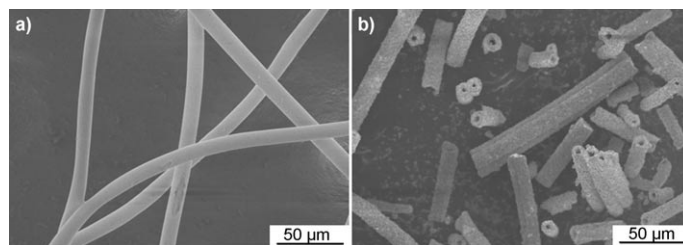


Figure 2. SEM images of a) ZrO_2 fibers and b) the as-grown TiO_2 tubular structures obtained from hydrothermal processing at 200°C for 24 h.

of the open ends and the surfaces of the as-prepared TiO_2 tubular structures. The latter are composed of many TiO_2 microcrystals and have external diameters of about $10\text{--}15\ \mu\text{m}$ and a wall thickness of approximately 3 μm . The high-magnification SEM image (Figure 3c) shows that the tubular structures consist of plate-shaped rectangular structures with side lengths of approximately 3 μm and thickness of approximately 1 μm . High-resolution transmission electron microscopy (HR-TEM) shows the (200) and (020) atomic planes with a lattice spacing of 0.19 nm (Figure 3d). The selected-area electron diffraction (SAED) patterns further confirm the single-crystalline characteristics, and the SAED pattern can be indexed as a (001) zone (insert of Figure 3d). In contrast to the case of regular anatase TiO_2 crystals, which are usually dominated by the thermodynamically stable {101} facets,^[21] both {101} and {001} facets are clearly observed in the microcrystallites of as-prepared TiO_2 tubular structures. The appearance of highly reactive {001} facets, which is thermodynamically unstable due to its higher surface energy, is due most probably to the F^- ions generated during the hydrothermal procedure, because F^- ions are known to preferentially stabilize the (001) rather than the (101) surface.^[20,21] The existence of F in the EDS (the inset of Figure 1) indicates that some F atoms are adsorbed on the TiO_2 microcrystal surfaces, thereby stabilizing the {001} facets. Based on the SEM image of the rectangular TiO_2 microcrystals, the percentage of the highly reactive {001} facets is estimated to be approximately 46%.

The synthesis of TiO_2 tubular structures by the hydrothermal process can be explained in terms of two reactions

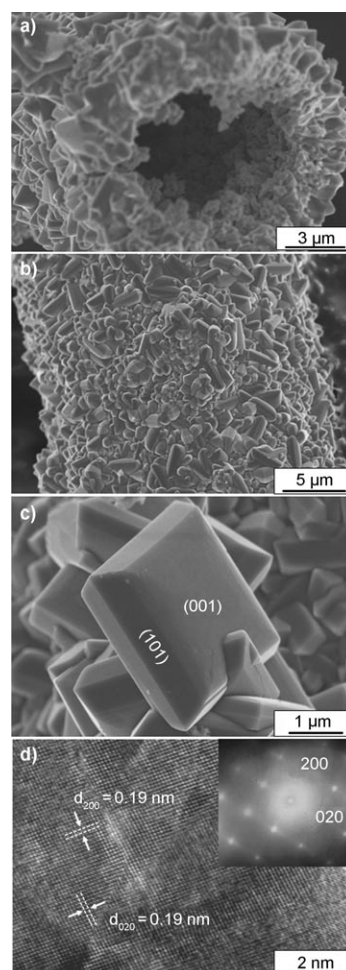
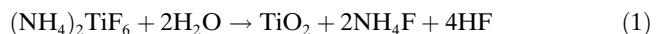


Figure 3. SEM images of anatase TiO_2 tubular structures: a) The end of one tube, b) the surface of a tube, and c) the faces of microcrystals. d) HR-TEM images of a TiO_2 sheet (the inset shows the corresponding SAED pattern).

shown in [Eq. (1)] and [Eq. (2)]. First, $(\text{NH}_4)_2\text{TiF}_6$ is hydrolyzed to form TiO_2 nanoparticles, HF and NH_4F [Eq. (1)]. Second, ZrO_2 fibers are gradually corroded away by the resulting HF and NH_4F and are transformed to water-soluble $(\text{NH}_4)_2\text{ZrF}_6$ [Eq. (2)].



In this way, TiO_2 nanoparticles are deposited and grow on the surfaces of ZrO_2 fibers, whereas the ZrO_2 fibers are gradually corroded as the reaction time t increases. Figure 4 illustrates the schematic diagram of a plausible growth mechanism, along with the cross-sectional SEM images of TiO_2 tubular structures obtained after hydrothermal processing at 200°C at various reaction times t . At $t=1$ h (Figure 4b), a dense layer of TiO_2 nanocrystals are randomly deposited on the smooth surfaces of ZrO_2 fibers. At $t=6$ h (Figure 4c), the TiO_2 layer grows thicker and the ZrO_2 tem-

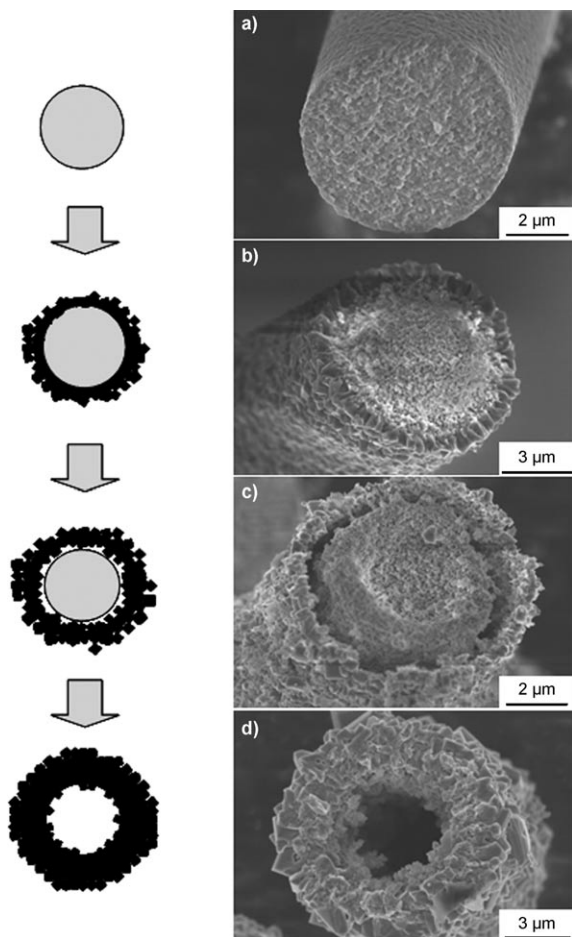


Figure 4. Schematic diagrams (left) illustrating the growth mechanism, which are consistent with the SEM images of TiO_2 microtubes obtained in a $(\text{NH}_4)_2\text{TiF}_6$ solution at 200°C for a) $t=0\text{ h}$, b) $t=1\text{ h}$, c) $t=6\text{ h}$, and d) $t=24\text{ h}$.

plates begin to corrode (Figure 4c). When t reaches 24 h (Figure 4d), the ZrO_2 templates are completely corroded away and only a TiO_2 tubular structure remains. Our analysis suggests that by controlling the morphologies and sizes of ZrO_2 templates a variety of anatase TiO_2 tubular or hollow spherical materials consisting of microcrystallites with high percentage of $\{001\}$ facets can be obtained.

In summary, we have developed a simple one-step hydrothermal template process for preparing TiO_2 tubular materials made up of microcrystallites with a high percentage of reactive $\{001\}$ facets, and have formulated a plausible growth mechanism for this process. The modification of the morphologies and sizes of ZrO_2 templates can lead to various anatase TiO_2 tubular or spherical materials made up of microcrystallites with a high percentage of $\{001\}$ facets, which can be of potential use in many fields.

Experimental Section

For the fabrication of anatase TiO_2 tubular structures composed of microcrystallites, tetragonal ZrO_2 polycrystalline fibers ($5\text{--}10\text{ }\mu\text{m}$ in diameter and longer than $\approx 50\text{ mm}$) were employed as a template in our experiments (as shown in Figure 1a). The fibers were pretreated by dipping them in dilute HNO_3 solution for about 12 h. Then they were filtered, rinsed with distilled water and ethanol three times, and dried at 80°C for 12 h in air prior to use. 1.23 g of pretreated ZrO_2 fibers was immersed in 40 mL aqueous solutions containing $(\text{NH}_4)_2\text{TiF}_6$ (2.97 g, 0.015 mol). The mixture was then transferred into 60 mL Teflon-lined stainless-steel autoclaves and maintained at 200°C for 24 h. After the reaction, the products were filtered, rinsed with distilled water and ethanol several times, and dried in an oven at 80°C .

The XRD patterns were taken on a Bruker AXS D8 advance powder diffractometer with a $\text{CuK}\alpha$ X-ray tube, using filtered $\text{CuK}\alpha$ radiation over a 2θ range from 15 to 80° with a step size of 0.02° and a counting time of 0.1 sstep^{-1} . The EDS was taken on a HORIBA EMAX Energy EX-350 energy dispersive X-ray microanalyzer. The morphologies and structure were observed by SEM (Hitachi S-4800 microscopy) and HRTEM (JEOL JEM-2100).

Acknowledgements

This work was financially supported by the National Basic Research Program of China (973 Program, Grant 2007CB613302), the National Natural Science Foundation of China under Grants (Nos. 20973102, 50721002, and 10774091), the Program of Introducing Talents of Discipline to Universities in China (111 Program), and China Postdoctoral Science Foundation funded project (20090461200). M.-H.W. is thankful for the support by the Office of Basic Energy Sciences, Division of Materials Sciences, U.S. Department of Energy, under Grant DE-FG02-86ER45259.

Keywords: anatase • hydrothermal synthesis • titanium • tubular structures • zirconium

- [1] S. Iijima, *Nature* **1991**, *354*, 56–58.
- [2] W. P. Hoffman, H. T. Phan, P. G. Wapner, *Mater. Res. Innovations* **1998**, *2*, 87–96.
- [3] D. T. Bong, T. D. Clark, J. R. Granja, M. R. Ghadiri, *Angew. Chem.* **2001**, *113*, 1016–1041; *Angew. Chem. Int. Ed.* **2001**, *40*, 988–1011.
- [4] P. Wang, B. B. Huang, J. Y. Wei, X. Y. Qin, S. S. Yao, Q. Zhang, *Mater. Lett.* **2007**, *61*, 5255–5257.
- [5] G. P. Celata, M. Cumo, S. McPhail, G. Zummo, *Heat Fluid Flow* **2006**, *27*, 135–143.
- [6] J. P. Cheng, Y. J. Zhang and R. Y. Guo, *J. Cryst. Growth* **2008**, *310*, 57–61.
- [7] G. S. Huang, Y. F. Mei, D. J. Thurmer, E. Coric, O. G. Schmidt, *Lab. Chip* **2009**, *9*, 263–268.
- [8] C. Rosenfeld, C. Serra, C. Brochon, G. Hadzioannou, *Chem. Eng. Sci.* **2007**, *62*, 5245–5250.
- [9] R. Li, X. Y. Xiao, A. W. Czarnik, *Tetrahedron Lett.* **1998**, *39*, 8581–8584.
- [10] E. Kaneko, J. Isoe, T. Iwabuchi, S. Hoshi, K. Akatsuka, T. Yotsuyanagi, *Analyst* **2002**, *127*, 219–222.
- [11] J. X. Wang, X. W. Sun, H. Huang, Y. C. Lee, O. K. Tan, M. B. Yu, G. Q. Lo, D. L. Kwong, *Appl. Phys. A* **2007**, *88*, 611–615.
- [12] Y. P. Rakovich, S. Balakrishnan, J. F. Donegan, T. S. Perova, R. A. Moore, Y. K. Gun'ko, *Adv. Funct. Mater.* **2007**, *17*, 1106–1114.
- [13] J. J. Schneider, J. Engstler, S. Franzka, K. Hofmann, B. Albert, J. Ensling, P. Gütlich, P. Hildebrandt, S. Döpner, W. Pfleiging, B. Günther, G. Müller, *Chem. Eur. J.* **2001**, *7*, 2888–2895.
- [14] J. Q. Hu, Y. Bando, F. F. Xu, Y. B. Li, J. H. Zhan, J. Y. Xu, D. Goldberg, *Adv. Mater.* **2004**, *16*, 153–156.

- [15] N. Shi, G. Yin, H. B. Li, M. Han, Z. Xu, *New J. Chem.* **2008**, *32*, 2011–2015.
- [16] Z. J. Liang, A. S. Susha, *Chem. Eur. J.* **2004**, *10*, 4910–4914.
- [17] Z. Y. Liu, L. J. Ci, N. Y. Jin-Phillipp, M. Rühle, *J. Mater. Chem.* **2007**, *17*, 4619–4625.
- [18] G. Zou, Z. Liu, D. Wang, C. Jiang, Y. Qian, *Eur. J. Inorg. Chem.* **2004**, 4521–4524.
- [19] J. M. Macak, M. Zlamal, J. Krysa, P. Schmuki, *Small* **2007**, *3*, 300–304.
- [20] D. Q. Zhang, G. S. Li, X. F. Yang, J. C. Yu, *Chem. Commun.* **2009**, 4381–4383.
- [21] H. G. Yang, C. H. Sun, S. Z. Qiao, J. Zou, G. Liu, S. C. Smith, H. M. Cheng, G. Q. Lu, *Nature* **2008**, *453*, 638–641.
- [22] H. G. Yang, G. Liu, S. Z. Qiao, C. H. Sun, Y. G. Jin, S. C. Smith, J. Zou, H. M. Cheng, G. Q. Lu, *J. Am. Chem. Soc.* **2009**, *131*, 4078–4083.
- [23] X. G. Han, Q. Kuang, M. S. Jin, Z. X. Xie, L. S. Zheng, *J. Am. Chem. Soc.* **2009**, *131*, 3152–3153.
- [24] Z. K. Zheng, B. B. Huang, X. Y. Qin, X. Y. Zhang, Y. Dai, M. H. Jiang, M.-H. Whangbo, *Chem. Eur. J.* **2009**, *15*, 12576–12579.

Received: December 21, 2009

Published online: May 12, 2010